

# Composition and Function of Spider Glues Maintained During the Evolution of Cobwebs

Dharamdeep Jain,<sup>†</sup> Ci Zhang,<sup>†</sup> Lydia Rose Cool,<sup>‡</sup> Todd A. Blackledge,<sup>§</sup> Chrys Wesdemiotis,<sup>‡</sup> Toshikazu Miyoshi,<sup>†</sup> and Ali Dhinojwala<sup>\*,†</sup>

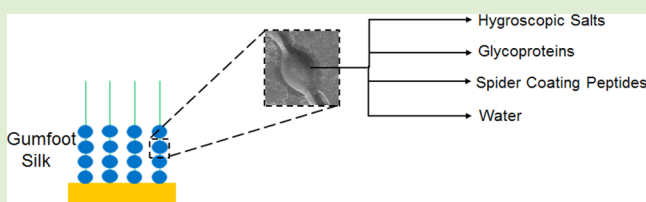
<sup>†</sup>Department of Polymer Science, The University of Akron, Akron, Ohio 44325-3909, United States

<sup>‡</sup>Department of Chemistry, The University of Akron, Akron, Ohio 44325-3601, United States

<sup>§</sup>Department of Biology, Integrated Bioscience Program, The University of Akron, Akron, Ohio 44325-3908, United States

## S Supporting Information

**ABSTRACT:** Capture silks are an interesting class of biological glues that help spiders subdue their prey. Viscid capture silk produced by the orb web spiders is a combination of hygroscopic salts that aid in water uptake and interact with adhesive glycoproteins to make them soft and sticky. The orb was a stepping stone to the evolution of new web types, but little is known about the adhesives in these webs. For instance, cobweb spiders evolved from orb-weaving ancestors and utilize glue in specialized sticky gumfoot threads rather than an elastic spiral. Early investigation suggests that gumfoot adhesives are quite different viscid glues because they lack a visible glycoprotein core, act as viscoelastic fluids rather than solids, and are largely invariant to humidity. Here, we use spectroscopic and staining methods to show that the gumfoot silk produced by *Latrodectus hesperus* (western black widow) is composed of hygroscopic organic salts and water insoluble glycoproteins, similar to viscid silk, in addition to a low concentration of spider coating peptides reported before. Our adhesion studies reveal that the organic salts play an important role in adhesion, similar to that seen in orb web spiders, but modulating function at much lower humidity. Our work shows more similarities in the viscid silk produced by orb web and cobweb spiders than previously anticipated and provide guidelines for developing synthetic adhesives that can work in dry to humid environments.



## INTRODUCTION

Biological adhesives<sup>1–3</sup> such as glues in a variety of aquatic animals,<sup>4–10</sup> keratin hairs in gecko setae,<sup>11</sup> and pollenkitt in pollen<sup>12</sup> maintain adhesion in the presence of water or humid environments<sup>13–15</sup> and in some cases even make strong bonds by displacing water from the contact interface,<sup>4,5</sup> a feat that has been hard to match using synthetic glues.<sup>16–21</sup> Hence, there is a strong need to understand the composition and mechanism of adhesion in biological materials with an ultimate goal to use those principles for fabricating synthetic adhesives that work in varying environmental conditions. Capture silks are produced by web building spiders to subdue their prey.<sup>22,23</sup> In the case of orb web spiders, the capture silk is known as “viscid silk” and consists of a bead-on-a-string morphology, where the thread is spun from silk produced in the flagelliform gland and the glue in the beads comes from the aggregate glands.<sup>22–24</sup> The aggregate secretions are a combination of glycosylated proteins,<sup>25–32</sup> termed ‘aggregate spider glue (ASG)’: ASG1 and ASG2,<sup>31,32</sup> and a range of hygroscopic, low molecular weight organic and inorganic salts that constitute ~70–80% of water-soluble mass.<sup>32</sup> The salts, such as GABamide, Betaine, Choline, *N*-acetyl taurine, KNO<sub>3</sub>, and KH<sub>2</sub>PO<sub>4</sub>, aid in water uptake that makes the silk tacky in humid conditions.<sup>32–40</sup> The salts also directly interact with and stabilize the glycoproteins.<sup>40</sup>

Many new web types evolved after the origin of aggregate glands that utilize viscid glue in novel ways.<sup>41</sup> One of the most dramatically different web type is the cobweb, built by a family of spiders known as *Theridiidae*.<sup>42–44</sup> The *Latrodectus* widow spiders are distributed worldwide in a variety of geographical zones and include well-known spiders like black widows, Australian red-backs and brown widows.<sup>44</sup> *Latrodectus hesperus* (western black widow) constructs three-dimensional cobwebs (Figure 1a) that use gumfoot threads that act as spring loaded traps adhering to walking prey. The aggregate adhesive silk is found only in the 0.5–2 cm lower portion of the gumfoot thread (Figure 1a,b), which is composed of an axial core of major ampullate silk.<sup>23,42,43</sup> This contrasts with the viscid silk of orb-weavers, where the aggregate glue is distributed all along a highly elastic, two-dimensional spiral of silk that targets mostly flying insects.<sup>23</sup> The aggregate secretions<sup>45</sup> form much larger glue droplets (Figure 1c) compared to viscid silk.<sup>46</sup> The composition of the “gumfoot silk” produced by cobweb spiders, is relatively unknown, although it does contain novel water-soluble spider coating peptides (SCP-1 and SCP-2).<sup>32,47</sup>

Received: August 2, 2015

Revised: August 25, 2015

Published: August 31, 2015

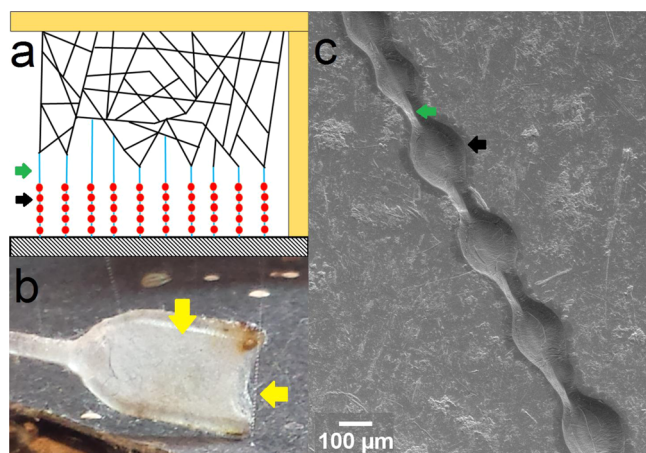


**Figure 1.** Arrangement and Collection of Gumfoot Silk. Panel a shows the schematic of a cobweb built by the western black widow (*Latrodectus hesperus*) where the gumfoot silk is present near the base of the web. The gumfoot silk thread is composed of beads of adhesive glue (black arrow) on a major ampullate silk thread (green arrow). Panel b shows the collection of gumfoot threads (yellow arrow) from the base of web by using a glass fork. Panel c is the SEM micrograph of a gumfoot silk thread (glue; black arrow and major ampullate silk; green arrow).

Cobweb spider glues appear functionally different from typical orb spider glues. Compared to the viscid silk produced by the orb spider *Larinioides cornutus*, *Latrodectus hesperus* gumfoot silk showed much weaker humidity response.<sup>46</sup> In addition, the viscid silk exhibited viscoelastic solid-like properties<sup>29</sup> where the stress did not relax completely with time while the gumfoot silk showed a viscoelastic liquid like properties, where the stress relaxed to values close to zero.<sup>46</sup> The glue droplets also lack the heterogeneous core that is visible at the centers of orb spider glue droplets. These differences in adhesive and structural properties suggest that aggregate secretions in cobwebs spiders many have evolved unique compositions. It is also unlikely that just a mixture of water and SCPs<sup>47</sup> are sufficient to impart strong adhesion in gumfoot silk. These observations raise the question of what else is present in these large glue droplets of gumfoot silk?

To answer this interesting concern, we used solution and solid-state nuclear magnetic spectroscopy (NMR), matrix assisted laser desorption ionization mass spectrometry (MALDI-MS), and staining to characterize the gumfoot silk produced by black widows. We also correlate that compositional analysis with how the thread adhesion changes as a function of humidity for both pristine and washed gumfoot silk threads. Our goal is to understand the material properties and the role it plays in the adhesion mechanism of capture silks, and offer insights in new ways to design synthetic bioinspired adhesives.

## MATERIALS AND METHODS

**Spider Care/Housing.** In order to collect gumfoot silk for studying the material and adhesion properties, about 40 adult female *Latrodectus hesperus* (western black widow) were purchased from Bugs of America (Arizona, USA) and housed in custom-built plastic cages lined with cardboard frames to promote cobweb building.<sup>42,43</sup> The spiders were fed with crickets twice weekly, and cages were misted with water once every week.

**Thread Adhesion.** Fresh individual silk strands of gumfoot were collected from the cobweb of *Latrodectus hesperus* directly onto cardboard cutouts across 5 mm gaps and adhered using Elmer's glue. Experiments were conducted using an MTS NanoBionix (Agilent) with

a custom designed environmental chamber. The silk was fixed on the upper clamp perpendicular to a 3 mm wide glass substrate placed on the lower clamp. To determine how adhesion changed as a function of humidity, the gumfoot silk was equilibrated at the desired humidity (10%, 30%, 50%, 70% and 90% R.H.) for 3 min and then brought in contact with glass substrates. The preload force was fixed at 50 mN, and, after contact for 6 s, the silk was pulled away at a rate of 0.1 mm/s and the detachment work/work of adhesion (stickiness) was calculated from the force–displacement measurements. A total of 15 samples were tested for each humidity condition for pristine gumfoot silk threads. To determine how water-soluble compounds influence adhesion, pristine silk was immersed in a water dish to remove the salts and peptides (water-soluble components) and dried in air overnight to produce washed gumfoot threads. Next, washed gumfoot threads were tested for their adhesion in different humidity environments as described above (five threads for each humidity). Treatments were compared using a one-way ANOVA, with Tukey HSD pairwise posthoc comparisons.

**Extraction of Water-Soluble Components from Gumfoot Strands.** To extract and analyze the water-soluble components, gumfoot silk strands were collected onto a custom built glass fork (Figure 1b). Silk threads were collected over a period of 6 months to yield five samples: 3000, 750, 450, 350, and 150 strands. Sample collections were done at room humidity (20–30% R.H.). The larger samples were used for solid-state NMR, while the smaller samples were used for less sample-intensive techniques like solution-state NMR. Each set of collected silk strands were washed with 10 mL of deionized water followed by lyophilization of the washed residue to procure the dried extract. The water-soluble extract was weighed and refrigerated until it was used for solution-state NMR and MALDI experiments. The washed gumfoot silk (silk after the removal of water-soluble components) was dried and preserved for the microscopy experiments.

**Solution-State NMR.** Solution-State NMR measurements were used to trace the presence of salts in the water-soluble extract. A part of the water-soluble extract was dissolved in 99.96% deuterated water (~1 mL) (Cambridge Isotope Laboratories) and packed in the 5 mm NMR tube (Norell) for analysis. To identify the peaks in the NMR spectra of water-soluble extract for salts, commercial standards of GABA, Isethionic Acid, and Choline Acetate (Sigma-Aldrich), and GABamide (provided by Dr. Townley, University of New Hampshire) were solubilized in deuterated water and packed in NMR tubes. Proton spin–lattice relaxation ( $T_1$ ) measurements were carried to determine the appropriate recycle delay for quantification experiments. The longest relaxation time (4 s) was for isethionic acid triplet peak around 3.8 ppm. The recycle delay was set to  $5 * T_1 \sim 20$  s for further natural extract experiments. <sup>1</sup>H NMR experiments were conducted for all samples at 298 K on a Varian Mercury 300 MHz spectrometer. The experiments were recorded with 128 scans for natural water-soluble extract with a delay of 20 s and a 90° pulse-width of 15.20 μs and acquisition time 3 s. The commercial salts spectra were recorded with 32 scans. The peaks were integrated using ACD/NMR software to calculate the relative composition.

**Matrix-Assisted Laser Desorption Ionization Time-of-Flight Mass Spectrometry (MALDI-ToF-MS).** We used mass spectroscopy to identify rare compounds in the glue. The water-soluble extract was dissolved in a minimal amount of water (Fisher, Optima grade), and 1 μg of trypsin (Sigma-Aldrich) was added to the solution. The samples were digested overnight at 37 °C. A solution of the matrix ( $\alpha$ -Cyano-4-hydroxycinnamic acid, CHCA) was prepared in methanol (Fisher, Optima grade) at a concentration of 10 g/mL. A layer of CHCA solution was added to the MALDI plate. The sample solution was filtered with a ZipTip (Millipore, C18) directly onto the MALDI plate. The water was allowed to evaporate before an additional layer of CHCA solution was applied. A Bruker Ultraflex III (Billerica, MA) MALDI ToF/ToF mass spectrometer was used for analysis. The mass spectra were acquired in positive mode. Tandem mass spectrometry (MS/MS) was performed using LIFT mode.<sup>47</sup>

**Glycoprotein Staining Studies.** Periodic Acid–Schiff (PAS) stain (Sigma-Aldrich) was used to determine where glycoproteins were present in the gumfoot strands. The standard protocol outlined by the supplier of the staining kit was followed for the experiments. The

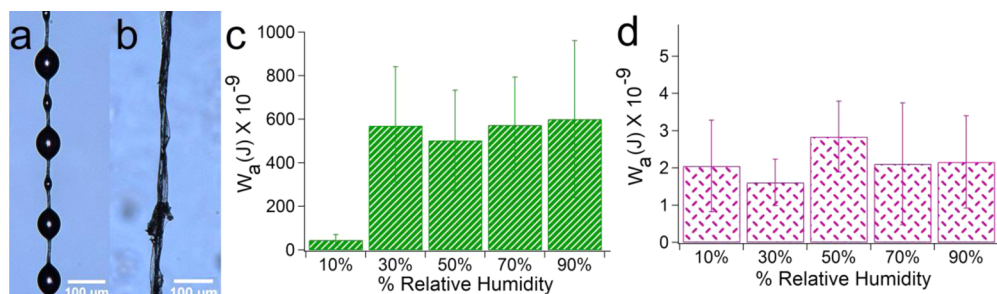


**Figure 2.** Adhesion measurements for pristine and washed gumfoot silk. Panels a and b depict the pristine and washed gumfoot silk threads. Panels c and d shows the variation of work of adhesion ( $W_a$ ) with relative humidity (% R.H.) ranging from 10%–90% for pristine and washed threads, respectively. The measured values are reported as  $\pm$  standard deviation.

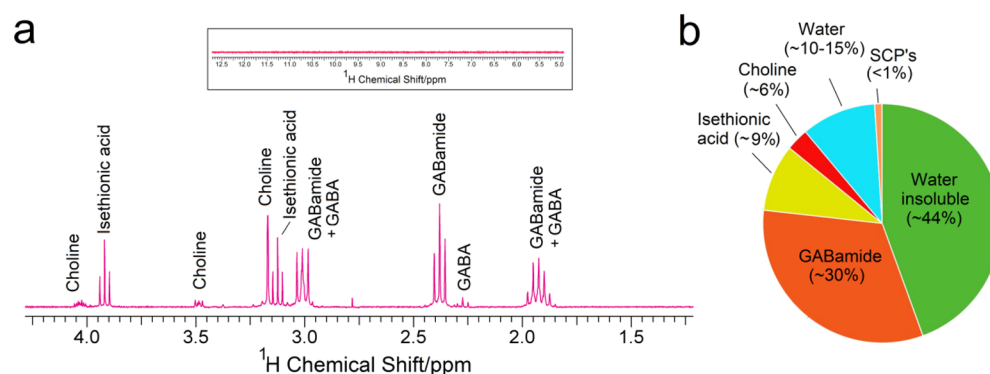


**Figure 3.** Composition of soluble components of gumfoot silk. Panel a is the  $^1\text{H}$  NMR spectrum for the water-soluble extract from gumfoot threads. Low molecular weight organic salts such as GABAmide, isethionic acid, and choline are clearly present in the extract, while no signatures of SCPs are detected. The inset in panel a shows the extended chemical shift range (5–12 ppm) depicting the absence of peptide peaks (SCPs) in the amide region. Panel b shows the different material components in the gumfoot silk relative to the total mass of collected gumfoot. Since GABA was found in only one of the five extracts analyzed, it is not included in the pie-chart. The water-soluble extract is  $\sim$ 56% of the total gumfoot silk mass and contains salts, water, and SCPs, while the water insoluble fraction  $\sim$ 44 wt % of the total mass contains residue along with major ampullate threads.

pristine gumfoot silk, pristine viscid silk, and reeled major ampullate silk threads were individually placed on glass slides. The slides were immersed in Periodic Acid solution for 5 min at 25 °C followed by rinsing in distilled water. Next, the slides were immersed in the Schiff's reagent for 15 min at 25 °C. After that, they were washed in running tap water for 5 min. The slides were counterstained in Hematoxylin solution Gill No. 3 for 90 s and then again washed with tap water. Finally, the samples were dehydrated and mounted to observe under the light microscope at different magnifications (Olympus BX60).

**Solid-State NMR.** To trace the glycoprotein signatures in the bulk gumfoot silk samples, solid-state NMR experiments were performed on pristine and washed silk samples. The sample for pristine silk consisted of  $\sim$ 3000 gumfoot strands collected on a glass fork from the cobweb. For the washed silk sample, a sample set of 1400 strands was collected separately and was washed with deionized water and dried. Major Ampullate silk acted as a control sample and was collected by forcibly reeling the silk directly from the gland of the spider (without any isotope feeding) as described by Jenkins et al.<sup>48</sup> All samples were collected at 30–40% R.H. and were refrigerated until used for the NMR experiments. *Pristine Gumfoot Silk:* The glass fork wrapped with the gumfoot strands ( $\sim$ 3000) was crushed in a mortar pestle. The crushed silk sample was then kept in a custom-built humidity chamber assembly for an hour at 30% R.H. and temperature of 25 °C. After the humidity optimization, it was subsequently packed in the 4 mm solid-state NMR rotor and sealed with Teflon tape and then loaded in the NMR set up for analysis. *Washed Gumfoot Silk:* The 1400 dried and water-washed gumfoot strands were crushed and subjected to a similar procedure for humidity optimization and packed in the NMR rotor as described above. *Major Ampullate Silk:* The collected spool of silk ( $\sim$ 23 mg) was exposed to 30% R.H. as described earlier and packed in the NMR rotor to make it ready for analysis. All experiments were performed on a Bruker AVANCE 300 MHz NMR equipped with a 4 mm double resonance VT

CPMAS probe at 298 K. The  $^1\text{H}$  and  $^{13}\text{C}$  carrier frequencies were 300.1 and 75.6 MHz, respectively. The MAS rate was set to  $6000 \pm 3$  Hz. The  $^{13}\text{C}$  chemical shift was referenced to the CH signal of adamantane (29.46 ppm) as an external reference. The 90° pulses for  $^1\text{H}$  and  $^{13}\text{C}$  were 4  $\mu\text{s}$ , while the recycle delay and contact time were 2 s and 2 ms, respectively. High-power two pulse phase modulation (TPPM) decoupling with a field strength of 56 kHz was applied to the  $^1\text{H}$  channel during an acquisition time of 41 ms. In order to improve the S/N ratio, the data presented was processed by truncating the FIDs after 20 ms and zero filling up to 8192 points.

**Optical and Scanning Electron Microscopy (SEM) Imaging.** Gumfoot silk (pristine and washed) was imaged using optical and electron microscopy to see how removal of aqueous components affected morphology. Optical images (Figures 2a,b and 4b) were collected using Leica DM LB2, and that of Figure 4a was collected using Olympus SZX16 at different magnifications. SEM micrographs (Figure 4c,d) were taken using a JEOL JSM-7401F field emission scanning electron microscope at different magnifications. The washed silk samples (Figure 4c: individual thread and Figure 4d: multiple threads scraped from washed glass pipet used for collecting Solution NMR sample) were sputter coated with silver particles and were placed on the aluminum stubs lined with conductive carbon tape.

## RESULTS

**Adhesion of Gumfoot Silk Threads.** Adhesion of pristine versus washed gumfoot threads on a glass substrate was compared across 10–90% R.H. (Figure 2). Humidity had a significant effect on adhesion ( $P < 0.00001$ ). The adhesion at 10% R.H. is always lower than other humidity conditions ( $p < 0.0005$  for each pair-wise comparison) due to the silk being dry and

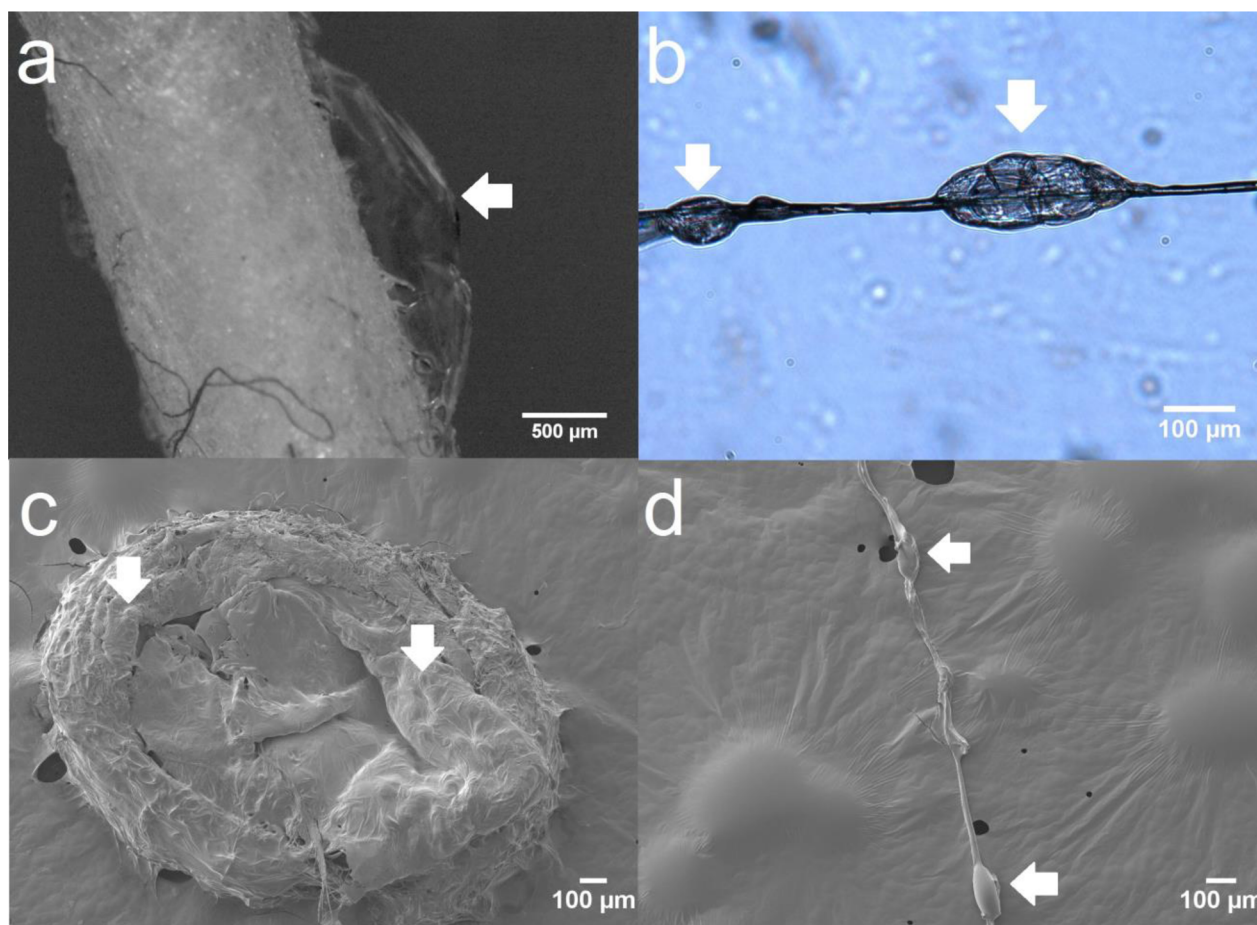


**Figure 4.** Residue on water-washed gumfoot silk threads. Panel a is an optical image of a bundle of washed gumfoot threads, while panel b is a single washed gumfoot silk thread. Panels c and d are the SEM micrographs of a number of washed threads scraped from the collection rod and single washed gumfoot silk thread, respectively. All the images show the presence of a residue (white arrow) left on the threads after a water-wash. Panels a and c (appears as residue blended with major ampullate fibers) show an agglomeration of the residue due to multiple threads in the sample.

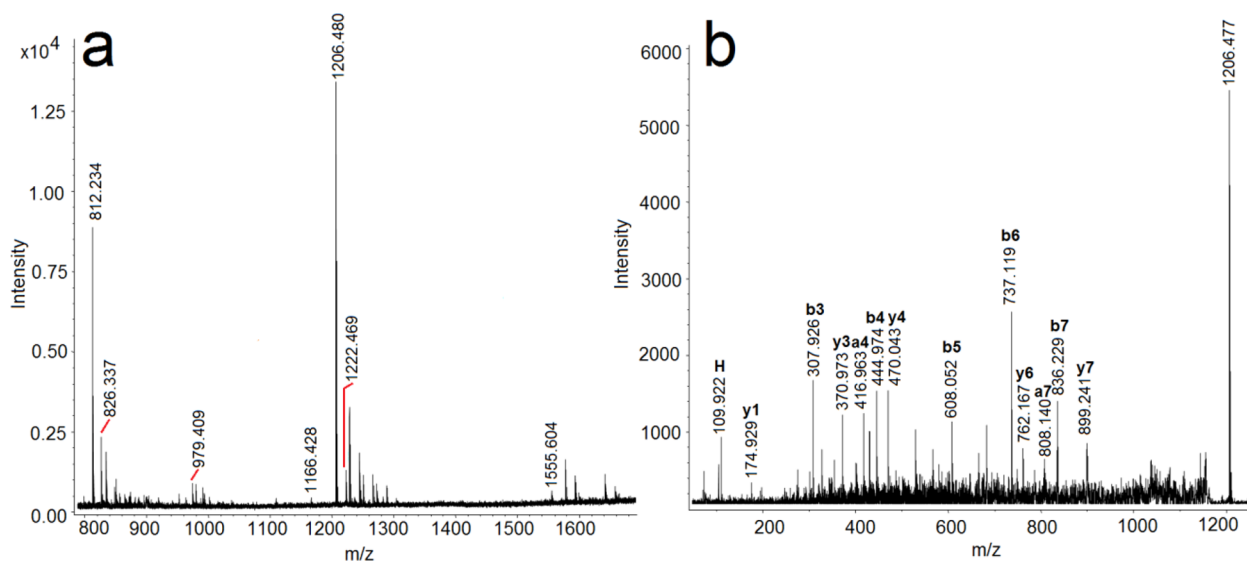


**Figure 5.** MALDI-ToF spectra of water washings from gumfoot silk. Spectrum a shows the fragments of trypsin digested water-soluble extract from gumfoot silk of *Latrodectus hesperus* highlighting the presence of peaks related to spider coating peptides (SCPs) particularly at  $m/z$  812.2, 826.3, 979.4, 1116.4, 1206.4, 1222.6, and 1555.5. Spectrum b is the CAD MS/MS of the 1206.4 peak showing the different fragments (labeled) corroborating the sequence AVHHYEVPR present in the SCPs.

unable to spread and adhere to the substrate. At 30% R.H. or higher, the adhesion was insensitive to humidity ( $p$ -value:

0.80–0.99). When the pristine silk was water-washed, the washed threads show no measurable stickiness across the

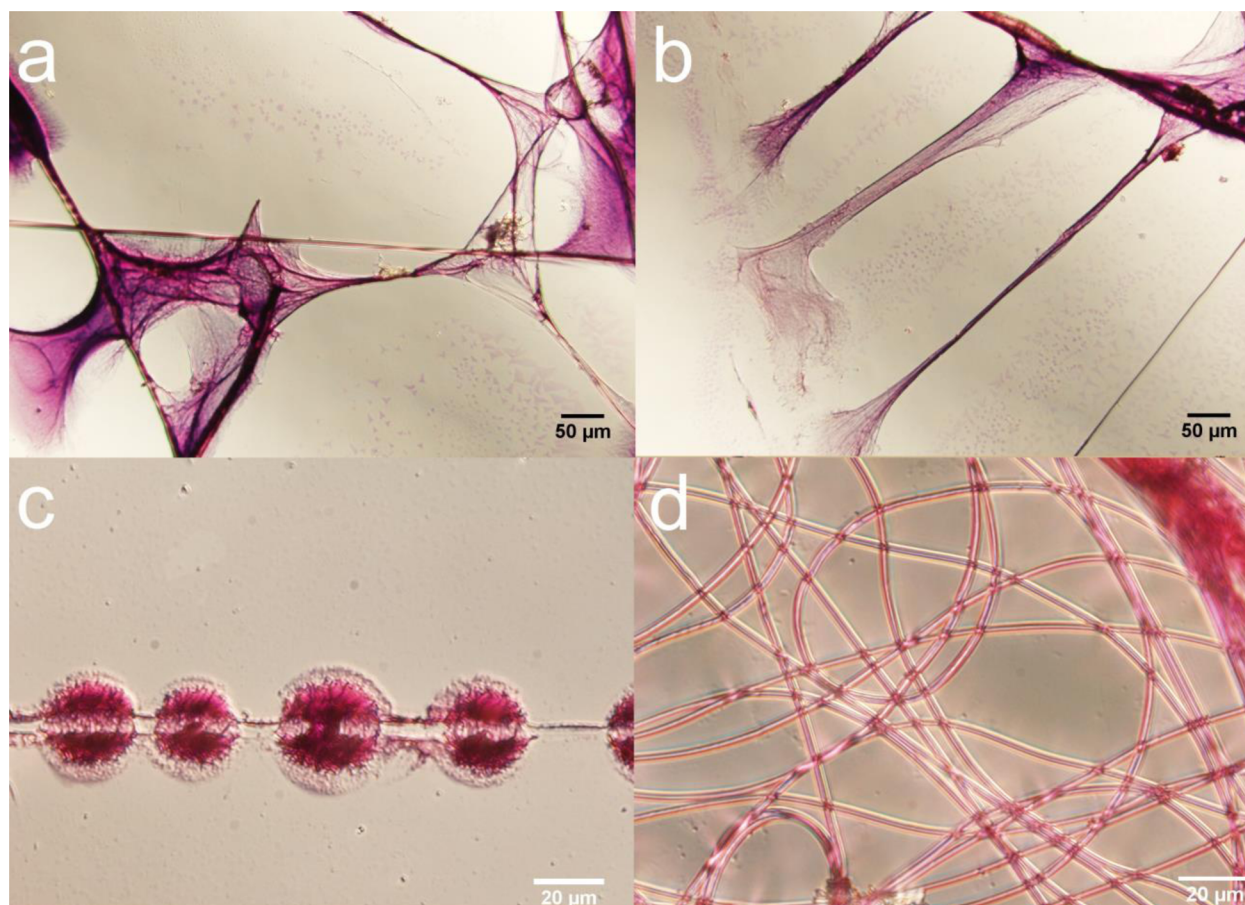


**Figure 6.** Periodic acid Schiff (PAS) staining. Panels show washed gumfoot silk from *Latrodectus hesperus* (a,b), washed viscid silk from the orb weaver *Larinioides cornutus* (c) (all immobilized on glass, water washed, and stained) and major ampullate silk (d) forcibly reeled from *Latrodectus hesperus* stained with PAS.

humidity range as compared to the pristine threads, indicating that the removal of water and water-soluble components drastically reduces the adhesive capability of gumfoot silk threads.

**Composition of Gumfoot Silk.** The water-soluble extract constituted  $\sim 56 \pm 12$  wt % of the mass of the collected gumfoot strands. Solution-state  $^1\text{H}$  NMR showed the presence of organic salts, which made up  $\sim 75$ – $85$  wt % of the water-soluble extract while the remaining portion was found to be made up of water ( $\sim 15$ – $25$  wt %, calculated using mass of the pristine gumfoot strands, washed gumfoot strands and water-soluble extract). The salt signatures consisted of GABamide ( $\sim 64 \pm 8$  wt %), isethionic acid ( $\sim 20 \pm 3$  wt %), and choline ( $\sim 14 \pm 5$  wt %). In one of five samples, traces of GABA ( $\sim 3\%$  wt %) were found. The NMR assignments were confirmed by analyzing commercially available salts (Supporting Information Figure 1) as well as from NMR spectra in the published silk literature.<sup>35,37,39,40</sup> SCPs (spider coating peptides)<sup>47</sup> were not detected in the water-soluble extract using  $^1\text{H}$  NMR, indicating that they must be less common even than the GABA salts.

The presence of an insoluble residue on the water-washed gumfoot silk thread (Figure 4) was striking and had not been reported in the published literature. This indicated an additional novel component in the gumfoot silk, besides previously reported SCPs<sup>47</sup> and presently discussed hygroscopic salts. However, the amount of the water insoluble residue could not be precisely determined due to the presence of major ampullate

threads in the sample (the remaining  $\sim 44$  wt % water insoluble part contains both insoluble residue and major ampullate silk). A summary of the various components present in the gumfoot silk is shown as a pie chart in Figure 3b.

**MALDI-ToF-MS of Water-Soluble Extracts from Gumfoot Silk.** We used MALDI-ToF-MS to confirm the presence of SCPs in the water-soluble extract because it is a more sensitive technique than solution-state NMR. Figure 5a shows the MALDI-ToF spectrum of trypsin-digested, washed-solution of the gumfoot silk of *Latrodectus hesperus*.

Many peptides identified were consistent with the earlier study by Hu et al.<sup>47</sup> The prominent peaks include  $m/z$  812.2, 826.2, 979.3, 1206.4, and 1555.5 corresponding to sequences TVHHYR, TIHHYR, HGLLNNVGR, AVHHYEVVPR, and TLFNQAADLLDHVV, respectively. Figure 5b is the MS/MS spectrum of the prominent peak ( $m/z$  1206.4) detected in the extract. Upon fragmentation, several product ions such as 109.9, 307.9, 370.9, 416.9, 444.9, 470.0, 608.0, 737.1, 762.1, 808.1, 836.2, and 899.2 were detected that correspond to different fragments of the AVHHYEVVPR peptide (as labeled in the spectrum). The absolute concentrations of the peptides could not be determined because of lack of controls to calibrate the mass spectrometry analysis. Although all these sequences of SCPs have been detected before,<sup>47</sup> this analysis shows that the SCPs are present in the washed-solution and, because the solution-state NMR is unable to detect them, the SCPs are much

rarer than the quantity of organic salts present in the gumfoot silk.

**Analysis of Water Insoluble Residue.** The large quantity of water-insoluble fraction in the gumfoot silk was surprising and had not been reported before. All the samples showed this residue (Figure 4, white arrow) on the washed gumfoot silk, indicating the presence of water-insoluble material in the gumfoot silk. This residue was also visible in the SEM analysis (Figure 4c–d). To establish the chemical nature of the residue, we characterized it using staining analysis and solid-state NMR.

(i). **Staining Analysis.** Since the viscid silk of orb-weaving spiders has glycoproteins that are responsible for adhesion, we checked the water-insoluble fractions of the gumfoot silk using stains positive for glycoproteins. PAS staining is used to detect polysaccharides as well as glycans and glycoproteins.<sup>26,49</sup> Figure 6a–f shows the immobilized silk threads (gumfoot, viscid, major ampullate) stained with PAS. The gumfoot silk (Figure 6a–d) shows the presence of dark pink to magenta color (PAS positive) over the silk thread and at the ends of the thread where the insoluble residue collects after water washing.

Viscid silk threads (*Larinoidea cornutus*) (Figure 6c) stain similarly, confirming the presence of glycoproteins. The glycoproteins in the immobilized viscid silk threads, unlike the gumfoot silk assume a circular shape and maintain their geometrical structure after washing. This observation supports the hypothesis that there are structural differences between the gumfoot and viscid silk due to physical/chemical cross-linking in the later.<sup>46</sup> Major ampullate silk (Figure 6d) stained positively because it has a thin layer of glycoprotein.<sup>50</sup>

(ii). **Solid-State NMR.** To further identify the chemical nature of the water-insoluble residue, we compared the CPMAS spectra for pristine gumfoot silk, washed gumfoot silk, and pristine reeled MA silk (Figure 7). If gumfoot glue was comprised solely of salts and SCPs (water-soluble components), then the washed

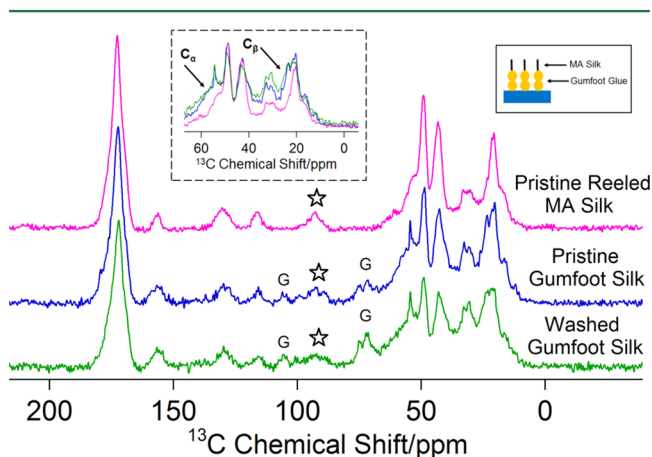


**Figure 7.** Identification of water insoluble residue with solid-state NMR. Figure shows the CPMAS (cross-polarization magic angle spinning) spectra for pristine reeled major ampullate silk, pristine gumfoot silk, and washed gumfoot silk. Inset schematic shows the arrangement of gumfoot silk (glue and MA silk). Ideally after washing, gumfoot silk and MA silk spectra should match if they are chemically identical, but the presence of a heightened shoulder around 25–35 ppm ( $C_{\beta}$  for amino acids), 55–60 ppm ( $C_{\alpha}$  for amino acids) (inset spectrum) and peaks related to glycoproteins (75 and 105 ppm, labeled as G) indicates the presence of additional proteinaceous residue in gumfoot silk that is absent in the control major ampullate silk sample. The starred peak refers to a spinning sideband. All spectra are measured at 30% R.H., 25 °C, and MAS frequency  $\sim$ 6 kHz.

gumfoot silk spectrum should resemble that of the major ampullate silk<sup>48</sup> (since the glue adheres to MA silk, Figure 7 schematic inset). However, key differences were observed in the spectrum of washed gumfoot silk. The heightened shoulders around 50–65 ppm and 25–30 ppm in the pristine and washed gumfoot silk (Figure 7, spectrum inset) corresponding to the  $C_{\alpha}$  and  $C_{\beta}$  signatures for amino acids, respectively,<sup>51</sup> hinted at the presence of additional protein-based molecules in the gumfoot silk as compared to major ampullate silk.

Further, an unidentified peak around 70–75 and 105 ppm was present in the spectra for pristine and washed gumfoot silk but absent in the major ampullate silk. Recent studies on caddisfly larval silk<sup>7</sup> using solid-state NMR showed these regions correspond to carbohydrate/glycosylated signatures. These observations confirm the presence of protein-based molecules, specifically glycoproteins, that are unique to the gluey regions of gumfoot threads.

## DISCUSSION

Spiders use the adhesive silk in their webs to capture prey.<sup>22,23</sup> The aggregate glues of orb spiders are complex mixes of glycoproteins<sup>25–32</sup> and cocktails of hygroscopic salts<sup>32–40</sup> that make the glues highly humidity responsive.<sup>40,46,52</sup> However, aggregate glues are used in new ways in many of the webs that evolved from orb-weaving ancestors.<sup>41</sup> Here, we report for the first time significant chemical similarities in the aggregate glues of cobweb spiders compared to their orb-weaving relatives. Water-soluble organic salts are a major component of the glue ( $\sim$ 45 wt % salts +  $\sim$  10 wt % water) of the gumfoot silk of *Latrodectus hesperus* (western black widow), while the previously reported SCPs<sup>47</sup> are found to be present in low amounts. These salts are necessary for adhesion and make gumfoot silk adhesion humidity-responsive, but only at very low R.H. compared to orb spiders. Glycoproteins are also present in the gumfoot glue droplets. Thus, evolution maintained the basic structural and functional design of aggregate glue across a major ecological transition in web construction highlighting the interplay between salts and glycoproteins for generating strong adhesion.

In addition to the water-soluble components (salts and SCPs), we detected a water insoluble residue on the washed gumfoot threads (Figure 4, white arrow). The presence of residue was surprising and not discussed in the published literature.<sup>32,45</sup> The insoluble residue was analyzed using glycoprotein-sensitive staining (Figure 6) and solid-state NMR (Figure 7) studies and consisted of carbohydrate-based signatures, specifically glycoproteins. This is reminiscent of other biological adhesives where glycoproteins form an important part of sticky secretions (as seen in insects, starfish, limpets, ticks, velvet worms, and caddisfly).<sup>3</sup> The presence of glycoproteins in the gumfoot silk is also supported by the detection of glycoproteins in other aggregate secretion known as black widow defensive secretion (BWDS) in genus *Latrodectus*.<sup>32,45</sup> BWDS produced from the “atypical” aggregate gland<sup>45</sup> during response to predators or prey capture, comprises high and intermediate (8–100 kDa) molecular glycoproteins. One of the glycoproteins (Glycoprotein A) is rich in *N*-acetylgalactosamine, threonine, serine and proline.<sup>45</sup> Similar observations have been made for the viscid silk, where residue is left after washing threads with water (Supporting Information Figure 2). The residue has been well characterized in the past and is composed of glycoproteins.<sup>25–32</sup> However, more detailed analysis will be required in the future for establishing the identity of this protein-based residue in gumfoot silk.

The importance of water-soluble components for adhesion is indicated by the comparison of whole thread adhesion for pristine and washed silk (Figure 2c,d). Pristine threads show 2 orders of magnitude higher adhesion than washed threads, where the SCPs and salts were removed. This highlights the interaction between proteins, SCPs, and salts in maintaining the stickiness of spider silk glues. Glycoproteins alone present in the washed threads fail to adhere to the glass substrate and do not respond to humidity. Instead, the hygroscopic salts absorb water from the atmosphere and interact with glycoproteins to make the silk adhesive. There is a significant increase in adhesion around 30% R.H., and the adhesion remains constant from 30% R.H. to 90% R.H. At 10% R.H., the silk is rigid and dry and fails to make contact and spread, leading to poor adhesion. At 30% R.H. and higher, the salts absorb water and make the glycoproteins tacky and sticky (solid-state NMR, unpublished results). Thus, the gumfoot adhesion of black widow spiders is insensitive to humidity after 30% R.H. The relative independence of adhesion from changes in humidity is consistent with the foraging habitat of Black Widows since they reside over a broad range of varied environments including dry to moist microhabitats.<sup>44</sup> The importance of water-soluble components in controlling adhesion is similar to our previous results for washed viscid silk (*Larinioides cornutus*).<sup>40</sup> For viscid silk produced by orb-web weaving spiders, it has also been observed that across the various species of spiders including *Larinioides cornutus* that the silk adhesion is optimum at a particular humidity condition. This optimum humidity where the adhesion is maximum correlated with the optimum foraging conditions of that particular species of spiders (Amarpuri et al., unpublished results). These results point out that the material composition of the water-soluble components is important for adhesion.

Our findings show that natural selection maintained the basic ground plan for spider aggregate glue over more than 200 million years and across a major ecological transition in web spinning.<sup>41</sup> Cobweb spiders originated from an early orb weaving ancestor in the Jurassic, but elaborated the two-dimensional orb web into a three-dimensional cobweb that uses gumfoot threads to target walking, rather than flying, insect prey.<sup>41</sup> Gumfoot silk is a composite arrangement of glue secreted on stiffer major ampullate thread,<sup>23,42,43</sup> compared to the relatively elastic flagelliform silk present in the axial fiber in orb spiders' viscid silk.<sup>24</sup> The glue in gumfoot silk appears homogeneous, coalesces, and spreads easily, behaving more like a viscoelastic liquid<sup>46</sup> at different levels of humidity, hinting at the absence of cross-linking in the system. On the other hand, the viscid silk acts as a viscoelastic solid,<sup>29</sup> shows a dense central core, suggesting physical and chemical cross-linking in the silk.<sup>46</sup> Despite these differences, we find here major similarities between the gumfoot and viscid silk. Like viscid silk,<sup>32</sup> the gumfoot silk has a mixture of soluble hygroscopic organic salts and insoluble glycoproteins in the glue. Gumfoot silk loses its adhesion when those salts are washed away, like viscid silk.<sup>40</sup> Finally, we also found that adhesion increases significantly with humidity, as seen in viscid silk, but only at low R.H. so that gumfoot adhesion is mostly invariant to humidity across a broad range of potential microhabitats.

The constant adhesion of gumfoot silk above 30% R.H. is a key difference to orb spiders' viscid silk, which typically improve in their adhesion as humidity increases initially, but then declines above some species-specific optimum humidity (Opell et al., Amarpuri et al., unpublished results). The whole thread adhesion results for gumfoot threads are consistent with the single drop

pulling measurements where Sahni et al.<sup>46</sup> observed that adhesion was independent of humidity (15%, 40% and 90% R.H.). This stark variation in the adhesive behavior between gumfoot and viscid silk can possibly be due to the difference in chemical nature of the salts and glycoproteins. Gumfoot silk from *Latrodectus hesperus* contains salts like GABamide (~70%), isethionic acid and choline. Choline is relatively hygroscopic but present in the lowest concentration while GABamide and isethionic acid are hygroscopic only above 50% R.H.<sup>35</sup> In contrast, viscid silk often contains substantial quantities of highly hygroscopic salts. The glycoproteins<sup>27–32</sup> in viscid silk hold potential sites for glycosylation and are anticipated to play important role in water retention, elasticity, adhesion properties of viscid silk.<sup>31</sup> It is likely that the glycoproteins in gumfoot silk have similar domains but that differences in composition and structure of glycoproteins and their interaction with salts results in the differences in adhesion between the two types of silk glues. A detailed analysis of the protein sequence is necessary to understand the differences in the glycoproteins in the gumfoot and viscid silks.

## CONCLUSION

We studied the adhesive gumfoot silk from the cobweb of *Latrodectus hesperus* (western black widow) to understand how its composition correlates with adhesion. Solution-state NMR showed the water-soluble component is mostly composed of organic salts like GABamide, isethionic acid and choline, with only low concentrations of spider coating peptides (SCPs). A water insoluble residue on water washed silk threads was characterized using staining and solid-state NMR and consisted of glycoprotein. Finally, whole thread adhesion measurements showed the importance of water-soluble components in adhesion and optimization of silk adhesion across a broad range of humidity >30% R.H. Our study highlights the recurring observation of how salts and proteins interact to produce the adhesion of spider capture silk and how that interaction modulates adhesion in different humidity environments, a lesson that provides clues for developing humidity responsive synthetic adhesive systems.

## ASSOCIATED CONTENT

### Supporting Information

Additional figures including <sup>1</sup>H solution state NMR spectrum for commercially available salts and optical images of washed viscid silk threads from *Larinioides cornutus*. The Supporting Information is available free of charge on the ACS Publications website at DOI: 10.1021/acs.biomac.5b01040.

(PDF)

## AUTHOR INFORMATION

### Notes

The authors declare no competing financial interest.

## ACKNOWLEDGMENTS

The authors would like to thank the National Science Foundation (NSF) for funding the project, Dr. M.A. Townley (University of New Hampshire) for providing GABamide, Dr. Donald Ott (Biology, University of Akron) for assistance in staining studies, Edward Laughlin for fabrication of humidity chamber, Jack Gillespie for capture silk collection probes, Venkat Reddy Dudipala and Chun Gao (Chemistry, University of Akron) for <sup>1</sup>H relaxation measurements, Gaurav Amarpuri for

the optical images in [Supporting Information Figure 2](#), Bill Hsiung for assistance in reeling major ampullate silk from Black Widow, Kaushik Mishra for help with lyophilization of extracts, and Prasad Raut for timely help in SEM imaging.

## REFERENCES

- (1) In *Biological Adhesives*; Smith, A.; Callow, J. A., Eds.; Springer: Berlin Heidelberg, 2006.
- (2) In *Biological Adhesive Systems: From Nature to Medical Applications*; Byern, J.; Grunwald, I., Eds.; Springer: Wien/New York, 2010.
- (3) Hennebert, E.; Maldonado, B.; Ladurner, P.; Flammang, P.; Santos, R. *Interface Focus* **2015**, *5*, 20140064.
- (4) Yu, M.; Hwang, J.; Deming, T. J. *J. Am. Chem. Soc.* **1999**, *121*, 5825–5826.
- (5) Sever, M. J.; Weisser, J. T.; Monahan, J.; Srinivasan, S.; Wilker, J. J. *Angew. Chem.* **2004**, *116*, 454–456.
- (6) Stewart, R. J.; Wang, C. S. *Biomacromolecules* **2010**, *11*, 969–974.
- (7) Addison, J. B.; Ashton, N. N.; Weber, W. S.; Stewart, R. J.; Holland, G. P.; Yarger, J. L. *Biomacromolecules* **2013**, *14*, 1140–1148.
- (8) Wang, C. S.; Stewart, R. J. *Biomacromolecules* **2013**, *14*, 1607–1617.
- (9) Alberts, E. M.; Taylor, S. D.; Edwards, S. L.; Sherman, D. M.; Huang, C.-P.; Kenny, P.; Wilker, J. J. *ACS Appl. Mater. Interfaces* **2015**, *7*, 8533–8538.
- (10) Gohad, N. V.; Aldred, N.; Hartshorn, C. M.; Jong Lee, Y.; Cicerone, M. T.; Orihuela, B.; Clare, A. S.; Rittschof, D.; Mount, A. S. *Nat. Commun.* **2014**, *5*, 4414.
- (11) Jain, D.; Stark, A. Y.; Niewiarowski, P. H.; Miyoshi, T.; Dhinojwala, A. *Sci. Rep.* **2015**, *5*, 9594.
- (12) Lin, H.; Gomez, I.; Meredith, J. C. *Langmuir* **2013**, *29*, 3012–3023.
- (13) Puthoff, J. B.; Prowse, M. S.; Wilkinson, M.; Autumn, K. *J. Exp. Biol.* **2010**, *213*, 3699–3704.
- (14) Niewiarowski, P. H.; Lopez, S.; Ge, L.; Hagan, E.; Dhinojwala, A. *PLoS One* **2008**, *3*, e2192.
- (15) Lin, H.; Lizarraga, L.; Bottomley, L. A.; Meredith, J. C. *J. Colloid Interface Sci.* **2015**, *442*, 133–139.
- (16) Comyn, J. In *Adhesives in Marine Engineering*; Weitzenböck, J. R., Ed.; Woodhead Publishing Limited: Cambridge, U.K., 2012; p 187.
- (17) Tan, K. T.; Vogt, B. D.; White, C. C.; Steffens, K. L.; Goldman, J.; Satija, S. K.; Clerici, C.; Hunston, D. L. *Langmuir* **2008**, *24*, 9189–9193.
- (18) Neuendorf, R. E.; Saiz, E.; Tomsia, A. P.; Ritchie, R. O. *Acta Biomater.* **2008**, *4*, 1288–1296.
- (19) Korta, J.; Mlyniec, A.; Uhl, T. *Composites, Part B* **2015**, *79*, 621–630.
- (20) White, C.; Tan, K. T.; Hunston, D.; Steffens, K.; Stanley, D. L.; Satija, S. K.; Akgun, B.; Vogt, B. D. *Soft Matter* **2015**, *11*, 3994–4001.
- (21) Schindler, M.; Koller, M.; Müller-Buschbaum, P. *ACS Appl. Mater. Interfaces* **2015**, *7*, 12319–12327.
- (22) Sahni, V.; Dhinojwala, A.; Opell, B. D.; Blackledge, T. A. In *Biotechnology of Silk*; Asakura, T.; Miller, T., Eds.; Biologically-Inspired Systems; Springer Netherlands: Dordrecht, 2014; p 203–215.
- (23) Sahni, V.; Blackledge, T. A.; Dhinojwala, A. *J. Adhes.* **2011**, *87*, 595–614.
- (24) Opell, B. D.; Hendricks, M. L. *J. Exp. Biol.* **2007**, *210*, 553–560.
- (25) Sinohara, H.; Tillinghast, E. K. *Biochem. Int.* **1984**, *9*, 315–317.
- (26) Tillinghast, E. K. *Naturwissenschaften* **1981**, *68*, 526–527.
- (27) Vollrath, F.; Tillinghast, E. K. *Naturwissenschaften* **1991**, *78*, 557–559.
- (28) Tillinghast, E. K.; Townley, M. A.; Wight, T. N.; Uhlenbruck, G.; Janssen, E. *MRS Online Proc. Libr.* **1992**, *292*, 9–23.
- (29) Sahni, V.; Blackledge, T. A.; Dhinojwala, A. *Nat. Commun.* **2010**, *1*, 19.
- (30) Amarpuri, G.; Chaurasia, V.; Jain, D.; Blackledge, T. A.; Dhinojwala, A. *Sci. Rep.* **2015**, *5*, 9030.
- (31) Choreshe, O.; Bayarmagnai, B.; Lewis, R. V. *Biomacromolecules* **2009**, *10*, 2852–2856.
- (32) Townley, M. A.; Tillinghast, E. K. In *Spider Ecophysiology*; Nentwig, W., Ed.; Springer Berlin Heidelberg: Berlin, Heidelberg, 2013; p 283–302.
- (33) Tillinghast, E. K.; Christenson, T. *J. Arachnol.* **1984**, *12*, 69–74.
- (34) Anderson, C. M.; Tillinghast, E. K. *Physiol. Entomol.* **1980**, *5*, 101–106.
- (35) Vollrath, F.; Fairbrother, W. J.; Williams, R. J. P.; Tillinghast, E. K.; Bernstein, D. T.; Gallagher, K. S.; Townley, M. A. *Nature* **1990**, *345*, 526–528.
- (36) Tillinghast, E. K.; Huxtable, R. J.; Watson, W. H.; Townley, M. A. *Comp. Biochem. Physiol.* **1987**, *88B*, 457–460.
- (37) Townley, M. A.; Bernstein, D. T.; Gallagher, K. S.; Tillinghast, E. K. *J. Exp. Zool.* **1991**, *259*, 154–165.
- (38) Townley, M. A.; Tillinghast, E. K.; Neefus, C. D. *J. Exp. Biol.* **2006**, *209*, 1463–1486.
- (39) Townley, M.; Pu, Q.; Zercher, C. K.; Neefus, C. D.; Tillinghast, E. K. *Chem. Biodiversity* **2012**, *9*, 2159–2174.
- (40) Sahni, V.; Miyoshi, T.; Chen, K.; Jain, D.; Blamires, S. J.; Blackledge, T. A.; Dhinojwala, A. *Biomacromolecules* **2014**, *15*, 1225–1232.
- (41) Blackledge, T. A.; Scharff, N.; Coddington, J. A.; Szüts, T.; Wenzel, J. W.; Hayashi, C. Y.; Agnarsson, I. *Proc. Natl. Acad. Sci. U. S. A.* **2009**, *106*, 5229–5234.
- (42) Blackledge, T. A.; Summers, A. P.; Hayashi, C. Y. *Zoology* **2005**, *108*, 41–46.
- (43) Blackledge, T. A.; Swindeman, J. E.; Hayashi, C. Y. *J. Exp. Biol.* **2005**, *208*, 1937–1949.
- (44) Garb, J. E.; González, A.; Gillespie, R. G. *Mol. Phylogenet. Evol.* **2004**, *31*, 1127–1142.
- (45) Kelly, S. L. MS Thesis, University of New Hampshire, Durham, 1989.
- (46) Sahni, V.; Blackledge, T. A.; Dhinojwala, A. *Sci. Rep.* **2011**, *1*, 41.
- (47) Hu, X.; Yuan, J.; Wang, X.; Vasanthavada, K.; Falick, A. M.; Jones, P. R.; La Mattina, C.; Vierra, C. A. *Biochemistry* **2007**, *46*, 3294–3303.
- (48) Jenkins, J.; Sampath, S.; Butler, E.; Kim, J.; Henning, R. W.; Holland, G. P.; Yarger, J. L. *Biomacromolecules* **2013**, *14*, 3472–3483.
- (49) Wilson, N. L.; Karlsson, N. G.; Packer, N. H. In *Separation Methods in Proteomics*; Smejkal, G. B.; Lazarev, A., Eds.; CRC Press: Boca Raton, FL, 2005; p 350.
- (50) Augsten, K.; Mühlig, P.; Herrmann, C. *Scanning* **2000**, *22*, 12–15.
- (51) Wishart, D. S.; Bigam, C. G.; Holm, A.; Hodges, R. S.; Sykes, B. D. *J. Biomol. NMR* **1995**, *5*, 67–81.
- (52) Opell, B. D.; Karinshak, S. E.; Sigler, M. A. *J. Exp. Biol.* **2013**, *216*, 3023–3034.